Research Article | Vol. 25, No. 9 | 1 May 2017 | OPTICS EXPRESS 10312

Optics EXPRESS

Precision measurement of X-axis stage mirror profile in scanning beam interference lithography by three-probe system based on bidirectional integration model

ZHAOWU LIU,[1,2] SHAN JIANG,[1] XIAOTIAN LI,[1] YING SONG,[1] WENHAO LI,[1,3] AND BAYANHESHIG[1,4]

[1]*Changchun Institute of Optics, Fine Mechanics and Physics, Chinese Academy of Sciences, Changchun Jilin 130033, China*
[2]*University of Chinese Academy of Science, Beijing 101408, China*
[3]*liwh@ciomp.ac.cn*
[4]*bayin888@sina.com*

Abstract: A profile of an X-axis stage mirror results in a phase error of gratings in Scanning Beam Interference Lithography. Traditional methods of measuring the profile require extra probes and another large stage mirror on Y-axis, or requires other operations such as rotating measured object to adjust the zero-adjustment errors. This paper introduces a three-probe system removing the need for Y-axis optical path structure and proposes a bidirectional integration model to solve the problem of zero-adjustment error, simplifying the optical path structure and the measurement process. This method is confirmed by theoretical analysis and experimental results, which is better than traditional methods and can also be used in other application fields of three-point method.

OCIS codes: (120.0120) Instrumentation, measurement, and metrology; (120.3180) Interferometry; (120.4640) Optical instruments; (120.6650) Surface measurements, figure; (050.2770) Gratings.

References and links

1. H. Yu, X. Li, J. Zhu, H. Yu, X. Qi, and S. Feng, "Reducing the line curvature error of mechanically ruled gratings by interferometric control," Appl. Phys. B **117**(1), 279–286 (2014).
2. Q. Zhou, X. Li, K. Ni, R. Tian, and J. Pang, "Holographic fabrication of large-constant concave gratings for wide-range flat-field spectrometers with the addition of a concave lens," Opt. Express **24**(2), 732–738 (2016).
3. M. Schumann, T. Bückmann, N. Gruhler, M. Wegener, and W. Pernice, "Hybrid 2D-3D optical devices for integrated optics by direct laser writing," Light Sci. Appl. **3**(6), 175 (2014).
4. R. K. Heilmann, C. G. Chen, P. T. Konkola, and M. L. Schattenburg, "Dimensional metrology for nanometre-scale science and engineering: towards sub-nanometre accurate encoders," Nat. Nanotechnol. **15**(10), 504 (2004).
5. J. C. Montoya, C. H. Chang, R. K. Heilmann, and M. L. Schattenburg, "Doppler writing and linewidth control for scanning beam interference lithography," J. Vac. Sci. Technol. B **23**(6), 2640–2645 (2005).
6. W. Cheng, J. Zhu, Y. Zhang, A. Zeng, and H. Huang, "Status and Development of Scanning Beam Interference Lithography System," Laser Optoelectronics Prog. **52**, 1–12 (2015).
7. S. Jiang, Bayanheshig, M. Pan, W. Li, and Y. Song, "An Accurate Method for Measuring Interference Fringe Period in Scanning Beam Interference Lithography System," Acta Opt. Sin. **35**, 55–64 (2015).
8. L. He, X. Wang, and M. Ma, "Non- Flatness Measurement of Wafer Stage Mirrors in a Step-and-Scan Lithographic Tool," Chin. J. Lasers **34**, 519–525 (2007).
9. J. Montoya, R. Heilmann, and M. Schattenburg, "Measuring two-axis stage mirror non-flatness using linear/angular interferometers," in *ASPE*(2004), pp. 382–385.
10. S. Kiyono, and W. Gao, "Profile measurement of machined surface with a new differential method," Precis. Eng. **16**(3), 212–218 (1994).
11. Z. Liu, W. Li, J. Wang, S. Jiang, Y. Song, M. Pan, and Bayanheshig, "Online detection of profile deviation for nano precision 2-D stage mirror," Opt. Precision Eng. **24**, 40–47 (2016).
12. Q. Lv, W. Li, Bayanheshig, Y. Bai, Z. Liu, and W. Wang, "Interferometric precision displacement measurement system based on diffraction grating," Chin. Opt. **10**(1), 39-50 (2016).
13. P. Yang, T. Takamura, S. Takahashi, K. Takamasu, O. Sato, S. Osawa, and T. Takatsuji, "Multi-probe scanning system comprising three laser interferometers and one autocollimator for measuring flat bar mirror profile with nanometer accuracy," Precis. Eng. **35**(4), 686–692 (2011).

#290141 https://doi.org/10.1364/OE.25.010312
Journal © 2017 Received 7 Mar 2017; revised 16 Apr 2017; accepted 17 Apr 2017; published 25 Apr 2017

Optics EXPRESS

14. Z. Q. Yin, and S. Y. Li, "High accuracy error separation technique for on-machine measuring straightness," Precis. Eng. **30**(2), 192–200 (2006).
15. J. Hwang, C. H. Park, W. Gao, and S. W. Kim, "A three-probe system for measuring the parallelism and straightness of a pair of rails for ultra-precision guideways," Int. J. Mach. Tools Manuf. **47**(7-8), 1053–1058 (2007).
16. P. Yang, T. Takamura, S. Takahashi, K. Takamasu, O. Sato, S. Osawa, and T. Takatsuji, "Development of high-precision micro-coordinate measuring machine: Multi-probe measurement system for measuring yaw and straightness motion error of linear stage," Precis. Eng. **35**(3), 424–430 (2011).
17. W. Gao, J. C. Lee, Y. Arai, C. H. Park, W. Gao, J. C. Lee, Y. Arai, and C. H. Park, "An Improved Three-Probe Method for Precision Measurement of Straightness Verbesserung der Drei-Sensoren-Methode für die Präzisions-Geradheitsmessung," Plattform Für Methoden Systeme Und Anwendungen Der Messtechnik **76**, 259–265 (2009).
18. P. Yang, T. Takamura, S. Takahashi, K. Takamasu, O. Sato, S. Osawa, and T. Takatsuji, "Calibration for multiple motion errors of X-Y table on micro-coordinate measuring machine (M-CMM) by utilizing multi-probe scanning method," Isupen **8**, 1–6 (2013).
19. W. Gao, J. Yokoyama, H. Kojima, and S. Kiyono, "Precision measurement of cylinder straightness using a scanning multi-probe system," Precis. Eng. **26**(3), 279–288 (2002).
20. H. Ma, C. Zhuang, and Z. Xiong, "Multipoint Recursive Sequential Three-point Method for On-machine Roundness Measurement," Procedia Cirp **31**, 459–464 (2015).
21. W. Gao, J. Yokoyama, S. Kiyono, and N. Hitomi, "A scanning multiprobe straightness measurement system for alignment of linear collider accelerator," Key Eng. Mater. **295**, 253–258 (2005).

1. Introduction

Scanning Beam Interference Lithography(SBIL) is a new type of large size holographic grating fabrication in recent years. It absorbs the advantages of mechanically ruling [1], holographic exposure [2] and direct laser writing [3]. The two small-size Gauss lights coincide at the grating substrate surface and generate interference fringes. A two-axis (x, y) air bearing stage is utilized to move the substrate in a step-and-scan fashion, stitching and exposing the interference fringe patterns in the photoresist in order to obtain the large size holographic gratings [4–7]. The stage position along the X axis (perpendicular to grating fringe) is determined by measuring the relative displacement between a reference mirror (which is stationary) and an X-axis stage mirror (which moves together with the stage). When patterning gratings via a parallel scan, the stage is scanned closely parallel to the Y axis. Since the stage mirror is scanned together with the stage, a profile of the stage mirror will be imprinted in the gratings, which results in a phase error whose amplitude is proportional to the current-location stage mirror profile [8, 9].

The two-point method is a traditional method of measuring a stage mirror profile [8–11]. It uses two probes to detect the profile heights at two adjacent points on the test surface. The difference of the two probe outputs can remove the influence of the translational error motion of the scanning stage. However, the yaw error motion of the scanning stage requires another two probes and a Y-axis stage mirror to detect on the vertical axis. The length of the Y-axis stage mirror is no less than 1700 mm if the length of the grating is 1500 mm. This stage mirror is costly and difficult to manufacture and install. Moreover, such a large stage mirror affects the performance and positioning accuracy of the air bearing stage. It is not necessary because the grating scale is sufficient to determine the stage position along the Y axis [12].

The three-point method, which uses three displacement probes [13–21], can eliminate the influence of both the translational error motion and the yaw error motion. It is widely used for measuring straightness and roundness profiles of cylinder workpieces [19, 20]. However, if the zero-adjustment errors of the probes are not adjusted precisely, it will yield a parabolic error term in the profile evaluation result of the three-point method. When measuring straightness profiles of cylinder workpieces, the cylinder can be rotated 180° and scanned by the probe units again after the first scanning to make an accurate zero adjustment [21]. The stage mirror is attached to the stage, cannot be rotated, and restricts the utilization of the three-point method in the field of measurement of the stage mirror profile.

In this work, we introduce a three-probe system into precise measurement of an X-axis stage mirror profile in SBIL and propose a new mathematical model for three-probe system,

Optics EXPRESS

which we named as bidirectional integration model. By using the three-probe system based on proposed bidirectional integration model, the problem of zero-adjustment error is solved without the need for the extra probes on Y-axis and the large Y-axis stage mirror, or the need for other operations such as rotating the X stage mirror. So the new three-probe system can largely simplify the optical path structure and the measurement process of SBIL. Correspondingly, the principle and some experimental results are also described in detail. This method can also be used in other application fields of three-point method.

2. Three-probe system based on bidirectional integration model

2.1 Three-point method

Figure 1(a) shows a schematic of the three-point method for measuring the stage mirror profile. In this method, the stage is scanned along the Y direction. Three laser interferometers (A, B, and C) are arranged along the Y direction. The stage mirror is measured at three different points labeled a, b, c, which are separated by a distance d. The laser interferometer can only perform relative measurement, which means the absolute zero value of the laser interferometer is unknown, as shown in Fig. 1(b). We called the difference between the absolute zero value and the actual zero value a zero-adjustment error. The zero-adjustment errors of the three laser interferometers are e_a, e_b, and e_c, respectively. Assume that the profile height along the scanning direction is $E_x(y_i)$ at sampling position y_i. The corresponding laser interferometer outputs $x_a(y_i)$, $x_b(y_i)$, and $x_c(y_i)$ can be expressed [17] as

$$x_a(y_i)=x(y_i)+E_x(y_i-d)-d\theta(y_i)-e_a. \tag{1}$$

$$x_b(y_i)=x(y_i)+E_x(y_i)-e_b. \tag{2}$$

$$x_c(y_i)=x(y_i)+E_x(y_i+d)+d\theta(y_i)-e_c. \tag{3}$$

where $x(y_i)$ is the translational error, and $\theta(y_i)$ is the yaw error of the scanning stage at y_i, i = 1,2…n. n is the sampling number of each interferometer over the entire scanning length. To eliminate the data processing error, set the sampling period to be d. When the entire measurement length is L, n can be calculated by $n = L/d$-2. The actual sampling number of the three interferometers on the stage mirror is $n + 2$, (i = 0,1…n + 1).

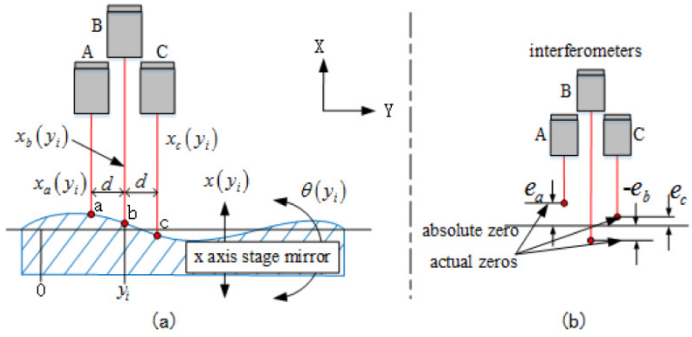

Fig. 1. Illustrative diagram of three-point method of stage mirror profile measurement: (a) schematic of three-point method and (b) zero-adjustment errors.

A quadratic differential output $f''(y_i)$ is calculated to remove the influence of the error motions:

$$f''(y_i)=\frac{x_c(y_i)-2x_b(y_i)+x_a(y_i)}{d^2}=\frac{E_x(y_i+d)-2E_x(y_i)+E_x(y_i-d)-\alpha}{d^2}. \tag{4}$$

Optics EXPRESS

where $\alpha = e_c\text{-}2e_b + e_a$. We get the quadratic differential of the profile function from the following equations:

$$E_x''(y_i) = \left(\frac{E_x(y_i + d) - E_x(y_i)}{d} - \frac{E_x(y_i) - E_x(y_i - d)}{d} \right) \frac{1}{d} = f''(y_i) + \frac{\alpha}{d^2}, i = 1, 2 \ldots n. \quad (5)$$

As is known, the profile of the stage mirror can be calculated from a double integration of $E_x''(y_i)$ as

$$E_x(y_i) = E_x(y_0) + \sum_{k=1}^{i} \left(E_x(y_0)' + \sum_{j=0}^{k-1} E_x''(y_j) d \right) d, \; i = 1, 2 \cdots n+1. \quad (6)$$

$E_x(y_0)$ is the profile height of the starting point y_0. Assume that $E_x(y_0) = 0$, $E_x'(y_0)$is the first differential of the starting point, and can be calculated as

$$E_x(y_0)' = \frac{x_b(y_1) - x_a(y_1)}{d} + \frac{\beta_{ab}}{d}. \quad (7)$$

where $\beta_{ab} = e_b\text{-}e_a$. By combining Eqs. (4)-(7), the profile of the stage mirror can be expressed as

$$E_x(y_i) = \begin{cases} 0, \; i = 0 \\ f(y_i) + \frac{\alpha}{2d^2}(y_i - y_1)^2 + \frac{\alpha}{2d}(y_i - y_1) + \frac{\beta_{ab}}{d} y_i, \; i = 1, 2 \cdots n+1 \end{cases}. \quad (8)$$

where $f(y_i)$ is the evaluated profile of the stage mirror calculated from the double integration of $f''(y_i)$, which is obtained from the interferometer outputs:

$$f(y_i) = \begin{cases} 0, \; i = 0 \\ E_x(y_0) + \sum_{k=1}^{i} \left(\frac{x_b(y_1) - x_a(y_1)}{d} + \sum_{j=0}^{k-1} f''(y_j) \delta \right) \delta, \; i = 1, 2 \cdots n+1 \end{cases}. \quad (9)$$

2.2 Zero adjustment

By inverting Eq. (8), the evaluated profile $f(y_i)$ deviated from the actual profile $E_x(y_i)$ can be expressed as

$$f(y_i) = \begin{cases} 0, i = 0 \\ E_x(y_i) - \frac{\alpha}{2d^2}(y_i - y_1)^2 - \frac{\alpha}{2d}(y_i - y_1) - \frac{\beta_{ab}}{d} y_i, i = 1, 2 \cdots n+1 \end{cases}. \quad (10)$$

A parabolic error term in the profile evaluation result is caused by α, and a linear error term is caused by α and β_{ab}. To clarify these coefficients, make y_{n+1} as starting point. The output data of the interferometer is integrated in the opposite direction using the same method.

$$f_{opposite}(y_i) = \begin{cases} E_x(y_{n+1}) = 0, i = n+1 \\ E_x(y_{n+1}) + \sum_{k=n}^{i} \left(-\frac{x_b(y_n) - x_c(y_n)}{d} + \sum_{j=n+1}^{k} f''(y_j) \delta \right) \delta, i = n, n-1 \cdots 0 \end{cases}. \quad (11)$$

The evaluated profile integrated in the opposite direction $f_{opposite}(y_i)$ and deviated from the actual profile $E_x(y_i)$ can be expressed as

Optics EXPRESS

$$f_{opposite}(y_i)=\begin{cases}E_x(y_i)-\dfrac{\alpha}{2d^2}(y_n-y_i)^2-\dfrac{\alpha}{2d}(y_n-y_i)+\dfrac{\beta_{bc}}{d}(y_{n+1}-y_i), i=0,2\cdots n\\ 0, i=n+1\end{cases}. \quad (12)$$

where $\beta_{bc} = e_c - e_b$. A comparison of the two calculation results indicates that they have the same parabolic errors but different linear errors. Subtract Eq. (10) from Eq. (12). The result removed the profile term and the parabolic error term, leaving a straight line:

$$\Delta f(y_i) = f_{opposite}(y_i) - f(y_i) = ky_i + b, i = 0,1\cdots n+1. \quad (13)$$

where

$$k = \frac{(n-1)\alpha}{d}. \quad (14)$$

$$b = -\frac{(n-2)(n+1)\alpha}{2} + (n+1)\beta_{ab}. \quad (15)$$

where $\alpha = \beta_{bc} - \beta_{ab}$ and $y_n/d = n$ are used in the calculation process. By inverting Eqs. (14) and (15), the coefficients are clarified:

$$\alpha = \frac{kd}{n-1}. \quad (16)$$

$$\beta_{ab} = \frac{b}{n+1} + \frac{(n-2)kd}{2(n-1)}. \quad (17)$$

By taking Eqs. (16) and (17) into Eq. (8), an accurate stage mirror profile can be evaluated.

3. Experiments

3.1 Experiments of three-point method

The experimental setup is shown in Fig. 2. An X-axis stage mirror with a length of 300 mm is attached to a two-axis stage in a clean laboratory. The stage mirror is parallel to the Y axis and used to help determining the stage position along the X axis. The stage is driven by a servomotor and has a travel range of 300 mm in both X and Y directions. Two Agilent 10721A Two-Axis Differential Interferometers and a reference mirror are attached to a granite platform, which is stationary. The measurements of the beams B and C are contributed by one interferometer, and that of the beam A is contributed by the other. The resolution of the Agilent 10721A series electronics is $\lambda/4/1024$, where λ = 632.8nm corresponds to the wavelength of a helium neon laser, and the factor of 4 is a result of the multiple passes in the beam path. Turning mirrors in the measuring path are used for alignment to make sure that measurement of beam A is parallel with B and C, and that the interval between A and B is equal to the interval between B and C. This interval is d = 12.7mm. A wavelength tracker is set to compensate the turbulence of the air refractive index. After adjustment, all devices are sealed in a cover. As the stage is scanned along the Y axis, the Y-directional displacement is detected by a HEIDENHAIN grating scale with a resolution of sub-μm. We collect a set of data every 12.7 mm (the sampling interval is set to 12.7 mm). We pause the stage to sample 2000 times at each sampling position in order to reduce the influence of noise. The number of sampling points of each interferometer is n = 21. The total number of sampling points is $n + 2$ = 23. The actual measured length of the stage mirror is $(n + 1) \times d$ = 279.4mm.

Optics EXPRESS

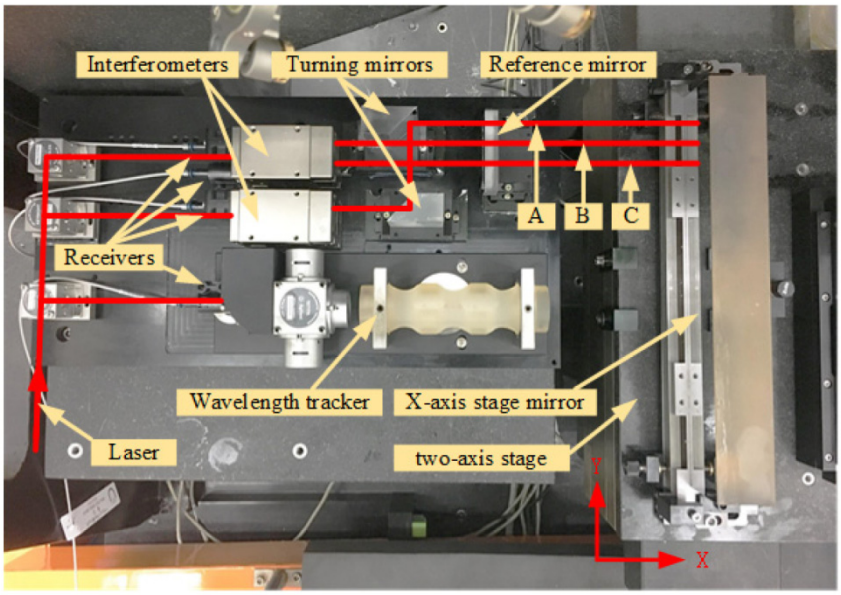

Fig. 2. Experimental setup of the three-point method.

The stage mirror profile is measured in two conditions; the difference between conditions is the installation mode of the stage mirror. Figure 3 shows the installation mode of the stage mirror for the first condition. Three Polytetrafluoroethylene (PTFE) blocks are installed to fix the stage mirror at the position of the red triangle in Fig. 3, named PTFE *d*, PTFE *e* and PTFE *f,* respectively. Firstly, PTFE *d* and PTFE *e* are installed on the mirror mount, then the X-axis stage mirror is put on the mirror mount press close to PTFE *d* and PTFE *e*, and finally PTFE *f* is screwed on the mirror mount to clamp the X-axis stage mirror. The results of the first condition are displayed in Fig. 4. Figure 4(a) presents the three interferometer outputs. The red line in Fig. 4(b) is obtained by double integration of the quadratic differential of the three interferometer outputs. The blue line is obtained by double integration in the opposite direction of the quadratic differential of the three interferometer outputs. The straight pink line indicates the difference between the two original evaluated profiles. The zero-adjustment errors are adjusted by Eqs. (16) and (17) using the information from the straight pink line: $\alpha = -1.0520$ and $\beta_{ab} = 26.8599$. By taking α and β_{ab} into Eq. (8), an accurate stage mirror profile can be evaluated. The experiment is conducted 20 times under the same conditions. Figure 4(c) shows a 20-times-evaluated profile with zero adjustment. The standard deviation of these 20 evaluated profiles is shown in Fig. 4(d). The repeatability of the stage mirror profile evaluation is no greater than 10 nm.

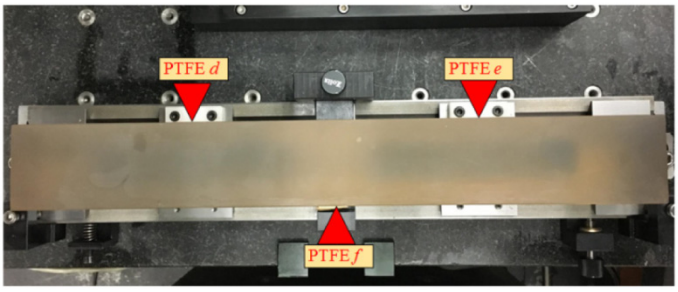

Fig. 3. Installation mode of stage mirror in the first condition.

Optics EXPRESS

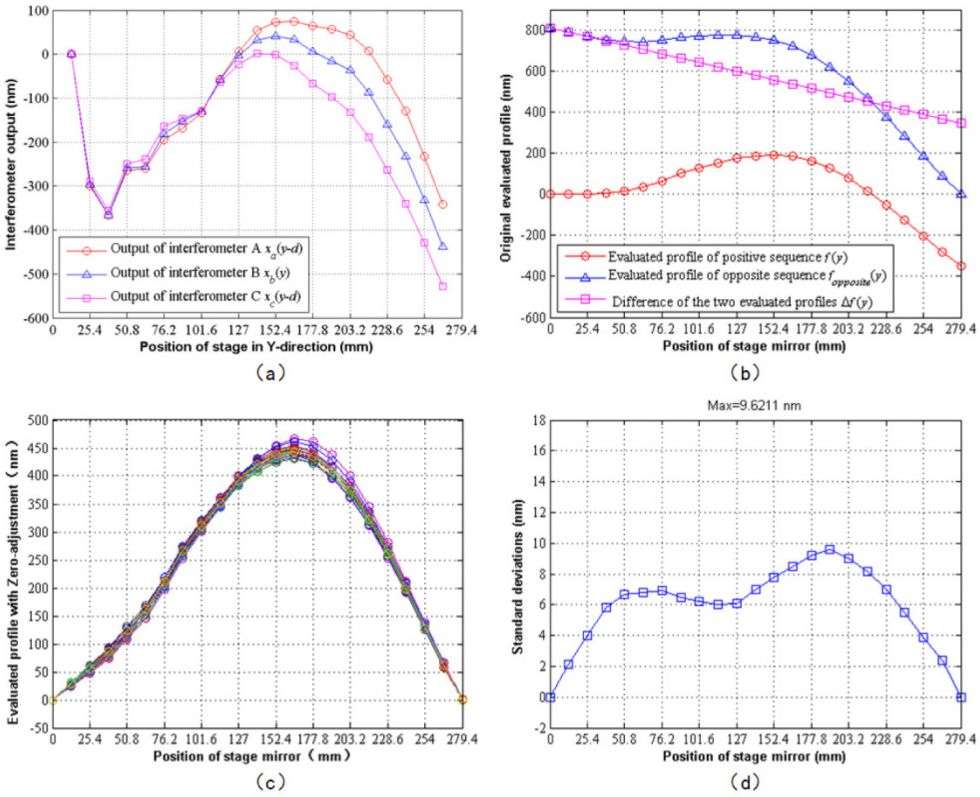

Fig. 4. Results of first condition: (a) interferometer outputs, (b) original evaluated profiles, (c) twenty-times-evaluated profile with zero adjustment, and (d) standard deviation of 20 times.

Figure 5 shows the installation mode of the stage mirror for the second condition. Four PTFE blocks are installed to fix the stage mirror at the position of the red triangle in Fig. 5, named PTFE *d*, PTFE *e*, PTFE *f* and PTFE *g, respectively*. Firstly, PTFE *d* and PTFE *e* are installed on the mirror mount, then the X-axis stage mirror is put on the mirror mount press close to PTFE *d* and PTFE *e*, and finally PTFE *f* and PTFE *g* are screwed on the mirror mount to clamp the X-axis stage mirror. The experiment is also conducted 20 times under the same conditions. Figure 6(a) displays the three interferometer outputs. Figure 6(b) presents the original evaluated profiles. Figure 6(c) shows the 20-times-evaluated profile with zero adjustment. The standard deviation of these 20 evaluated profiles is shown in Fig. 6(d). The repeatability of the stage mirror profile evaluation is no greater than 10 nm, which is the same as in the first condition.

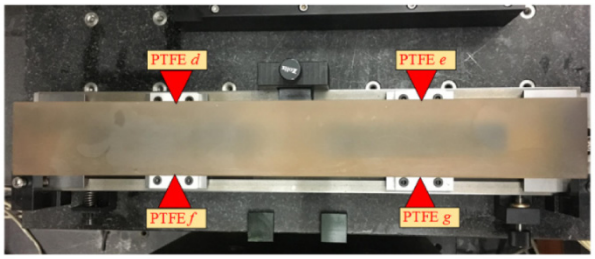

Fig. 5. Installation mode of stage mirror in the second condition.

Optics EXPRESS

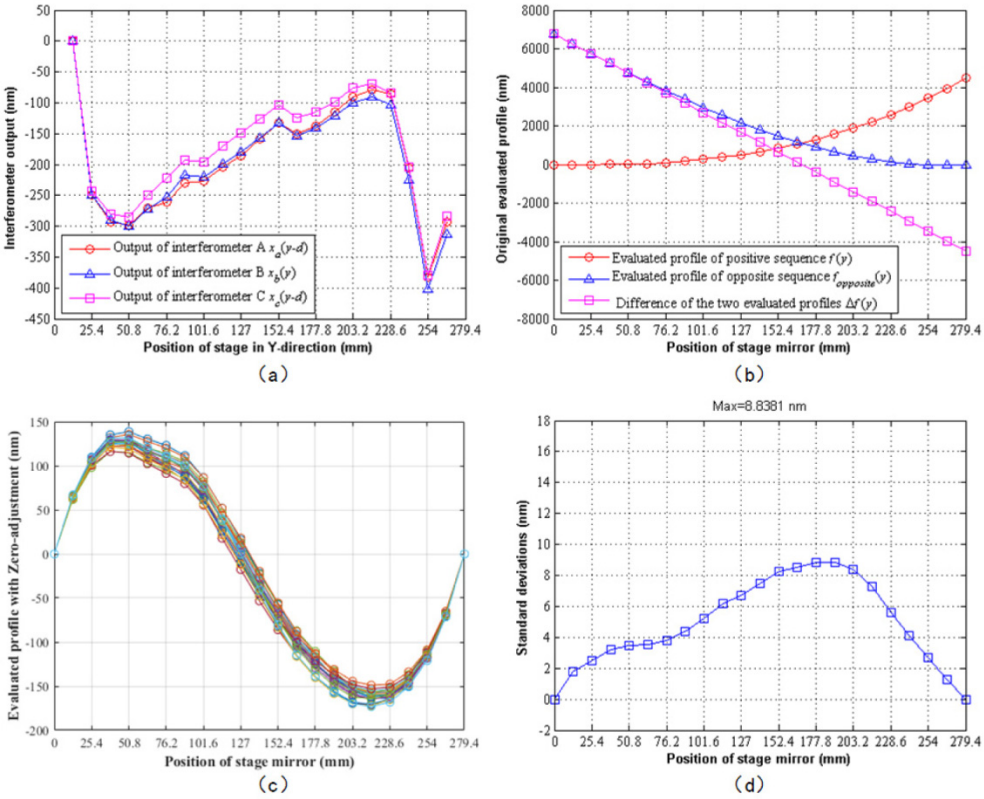

Fig. 6. Results of the second condition: (a) interferometer outputs, (b) original evaluated profiles, (c) twenty-times-evaluated profile with zero adjustment and (d) standard deviation of 20 times.

All the experimental results indicate that the different installation modes of the stage mirror have contributed to the different profiles, the stage mirror profile is presented as an arch when the stage mirror is fixed with three PTFE blocks, and as an S type when the stage mirror is fixed with four PTFE blocks. But the same repeatability accuracy of the stage mirror profile evaluation is obtained in the different installation modes.

3.2 Comparison experiment using two-point method

A comparison experiment using two-point method is set up in the first condition where three PTFE blocks are installed to fix X-axis stage mirror. X-axis measurement system is as same as experimental setup of three-point method; the details are shown in Fig. 2. Taking beams B and C as the two probes, the profile heights are detected. Well because beam A is not utilized, the total number of sampling points is $n + 1 = 22$ ($i = 1,2\ldots n + 1$). The actual measured length of the stage mirror is $n \times d = 266.7$mm.

Optics EXPRESS

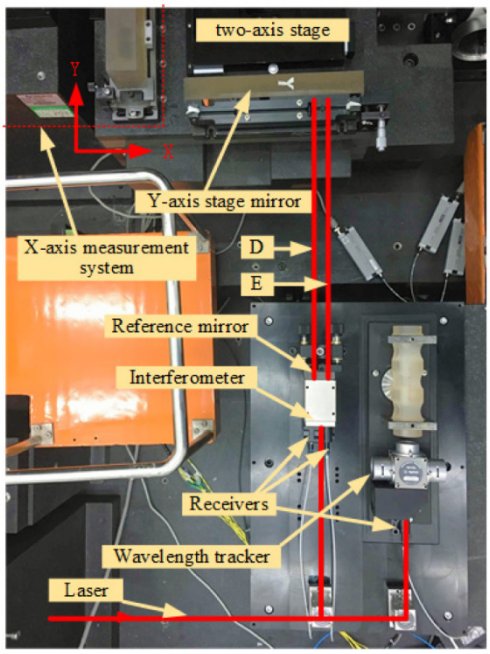

Fig. 7. Experimental setup of two-point method.

The Y-axis measurement system is shown in Fig. 7. A Y-axis stage mirror parallel to the X axis is attached to the stage. Another Agilent 10721A Two-Axis Differential Interferometers is used and attached to a granite platform together with a reference mirror. The measurements of beams D and E are used to detect the yaw error motion of the scanning stage, the corresponding laser interferometer outputs are $y_d(y_i)$, and $y_e(y_i)$, the interval between D and E is d = 12.7mm. In [10], the evaluated profile of the stage mirror using two-point method can be expressed as

$$E_x(y_i) = E_x(y_1) + \sum_{k=1}^{i-1}\left(\frac{x_c(y_i) - x_b(y_i)}{d} - \frac{y_e(y_i) - y_d(y_i)}{d}\right)\delta, i = 2, 2\cdots n+1. \quad (18)$$

The experiment is conducted 20 times under the same conditions. Figure 8(a) shows the 20-times-evaluated profile using the two-point method. The trend is accordant with Fig. 4(c); the little difference exists because there is a less sampling point in the comparison experiment. The standard deviation of these 20 evaluated profiles is shown in Fig. 8(b). The worst repeatability of the stage mirror profile evaluation is approximate 18 nm. The part of this error could be the result of air-refractive index variations, which are not corrected accurately during the acquisition of data by D and E, for the repeatability becomes worse as the state scanning farther away from the Y-axis measurement system.

All in all, the above analytical results indicate that the evaluated profile using the two-point method is accordant with the evaluated profile using the three-point method proved the feasibility of measuring a stage mirror profile by using three-probe system based on bidirectional integration model. Furthermore, the repeatability of the stage mirror profile evaluation using the three-point method is better than that using the two-point method.

Optics EXPRESS

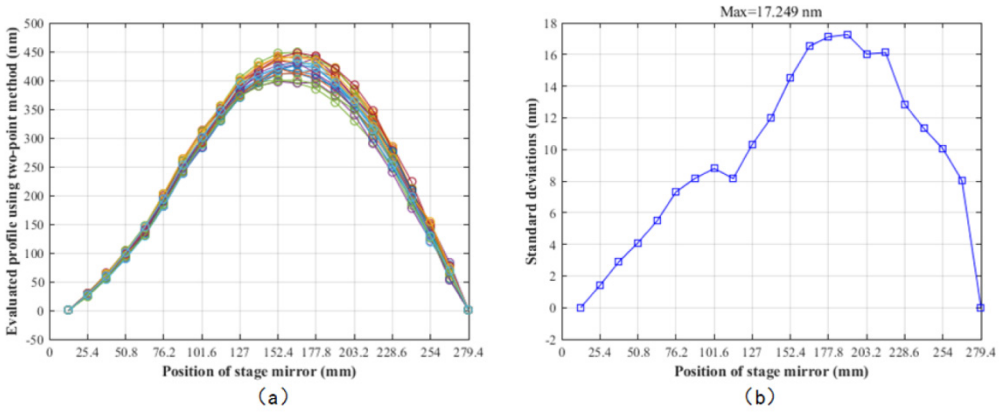

Fig. 8. Results of contrast experiment: (a) twenty-times-evaluated profile using two-point method and (d) standard deviation of 20 times.

4. Conclusions

We present a novel application of three-point method under a new mathematical model for precisely measuring a stage mirror profile using in Scanning Beam Interference Lithography. A quadratic differential output of the stage mirror profile is gathered using three interferometers. Double integration of the quadratic differential in the positive and opposite directions results in two original evaluated profiles with zero-adjustment errors. The zero-adjustment errors are adjusted by the difference between the two original evaluated profiles. Finally, an accurate stage mirror profile can be evaluated.

The experimental results indicate that the installation mode of the stage mirror has an impact on the stage mirror profile, the stage mirror profile is presented as an arch when the stage mirror is fixed with three PTFE blocks, and as an S type when the stage mirror is fixed with four PTFE blocks. And compared with the experiment using the two-point method, the profile by using the new three-probe system based on bidirectional integration model can be revealed availably, the repeatability of the stage mirror profile evaluation is no greater than 10 nm, better than that using the two-point method which is approximate 18 nm.

The part of this error could be the result of air-refractive index variations which are not corrected accurately during the acquisition of data. And there may be a little deformation on the stage mirror profile during scanning.

This method not only improves the accuracy of the stage position determine but also reduces the encumbrance of the air bearing stage by cutting down the Y-axis stage mirror. It is very significant of the big grating fabrication fields for improving the diffraction wave front of grating.

Funding

National Natural Science Foundation of China (NSFC) (grant no. 61227901, grant no.61505204), the Ministry of National Science and Technology for the National Key Basic Research Program of China (grant no. 2014CB049500) and Jilin Province Science & Technology Development Program Project in China (grant no. 20150203021GX, grant 20170520167JH).

Acknowledgments

We thank prof. Qi Chen for technical assistance of two-axis air bearing stage.